Cytotoxic (*cis,cis*-1,3,5-triaminocyclohexane)ruthenium(II)–diphosphine complexes; evidence for covalent binding *and* intercalation with DNA

Dan E. Wise,[a] Aimee J. Gamble,[b] Sham W. Arkawazi,[b,¶] Paul H. Walton,[b] M. Carmen Galan,[a] Michael P. O'Hagan,[a] Karen G. Hogg,[c] Joanne L. Marrison,[c] Peter J. O'Toole,[c] Hazel A. Sparkes,[a] Jason M. Lynam*[b] and Paul G. Pringle*[a]

[a]School of Chemistry, University of Bristol, Cantock's Close, Bristol, BS8 1TS, U.K.

[b]Department of Chemistry, University of York, Heslington, York, YO10 5DD, U.K.

[c]Imaging and Cytometry Laboratory, Bioscience Technology Facility, Department of Biology, University of York, U.K.

[¶]Current address, Department of Chemistry, University of Garmian, Kurdistan Region, Iraq.

Supplementary Information

Experimental 1
NMR Assignments 2
Synthesis of [RuCl(dmso-*S*)$_2$(κ^3-tach)]Cl, 1 3
Synthesis of 3',4'-bis(diphenylphosphanyl)-2,2':5',2''-terthiophene, L1 3
Synthesis of 2,3-dichlorodibenzo[f,h]quinoxaline 4
Synthesis of 2,3-bis(diphenylphosphino)dibenzo[f,h]quinoxaline, L3 4
Synthesis of [RuCl(dppbz)(κ^3-tach)]Cl, 3f 5
Synthesis of [RuCl(L1)(κ^3-tach)]Cl, 3g 6
Synthesis of [RuCl(L2)(κ^3-tach)]Cl, 3h 7
Synthesis of [RuCl(L3)(κ^3-tach)]Cl, 3i 8
Kinetics of Aquation 9
Determination of the pK_a of the Ru–OH$_2$ 10
Equilibrium of Aquation/Anation 11
Interactions with Nucleosides 13
Viability Assays 14
Competitive DNA Binding Studies 18
FRET G-Quadruplex Assay 20
LiveCyte Cell Imaging 22
X-Ray Crystallography 28
References 30

Experimental

Unless otherwise stated, all manipulations were carried out under an inert atmosphere (N_2) using standard Schlenk line techniques or in a glovebox (Ar). All glassware was oven-dried and cooled under vacuum prior to use. Unless otherwise stated, chemicals and reagents were purchased from commercial suppliers and used without further purification. Anhydrous solvents were obtained from an Anhydrous Engineering alumina column drying system based on the Grubbs design and degassed prior to use by sparging with nitrogen. All NMR spectra were acquired on Jeol ECS300, Jeol ECS400, Varian 400, Bruker 400 or Bruker CryoCarbon 500 MHz spectrometers. Chemical shifts (δ) are quoted in parts per million (ppm) and ^{1}H and $^{13}C\{^{1}H\}$ NMR spectra are referenced relative to the deuterated solvent. $^{31}P\{^{1}H\}$ NMR spectra are referenced relative to 85% H_3PO_4 as external standard. Mass spectrometry was carried out by the Mass Spectrometry Service, University of Bristol on either a VG Analytical Autospec (EI) or VG Analytical Quattro (ESI) spectrometer. X-ray crystallography was performed by the University of Bristol Crystallography Service using a Bruker Apex II diffractometer. Elemental analyses were performed by the University of York Microanalytical service.

The following compounds were prepared from literature procedures and spectroscopic data agreed with that reported:

$[RuCl_2(dmso\text{-}S)_3(dmso\text{-}O)]$[1], *cis*-diamminedichloroplatinum[2], *cis*-*cis*-1,3,5-triaminocyclohexane (*cis*-tach)[3], 3',4'-dibromo-2,2':5',2''-terthiophene[4], 2,3-bis(diphenylphosphino)quinoxaline[5] **L2**, 1,4-dihydrodibenzo[f,h]quinoxaline-2,3-dione[6], **[2a-c]**[7], **[3a-f]**[7].

NMR Assignments

For ruthenium complexes **3f-i**, the following NMR assignment labels are used:

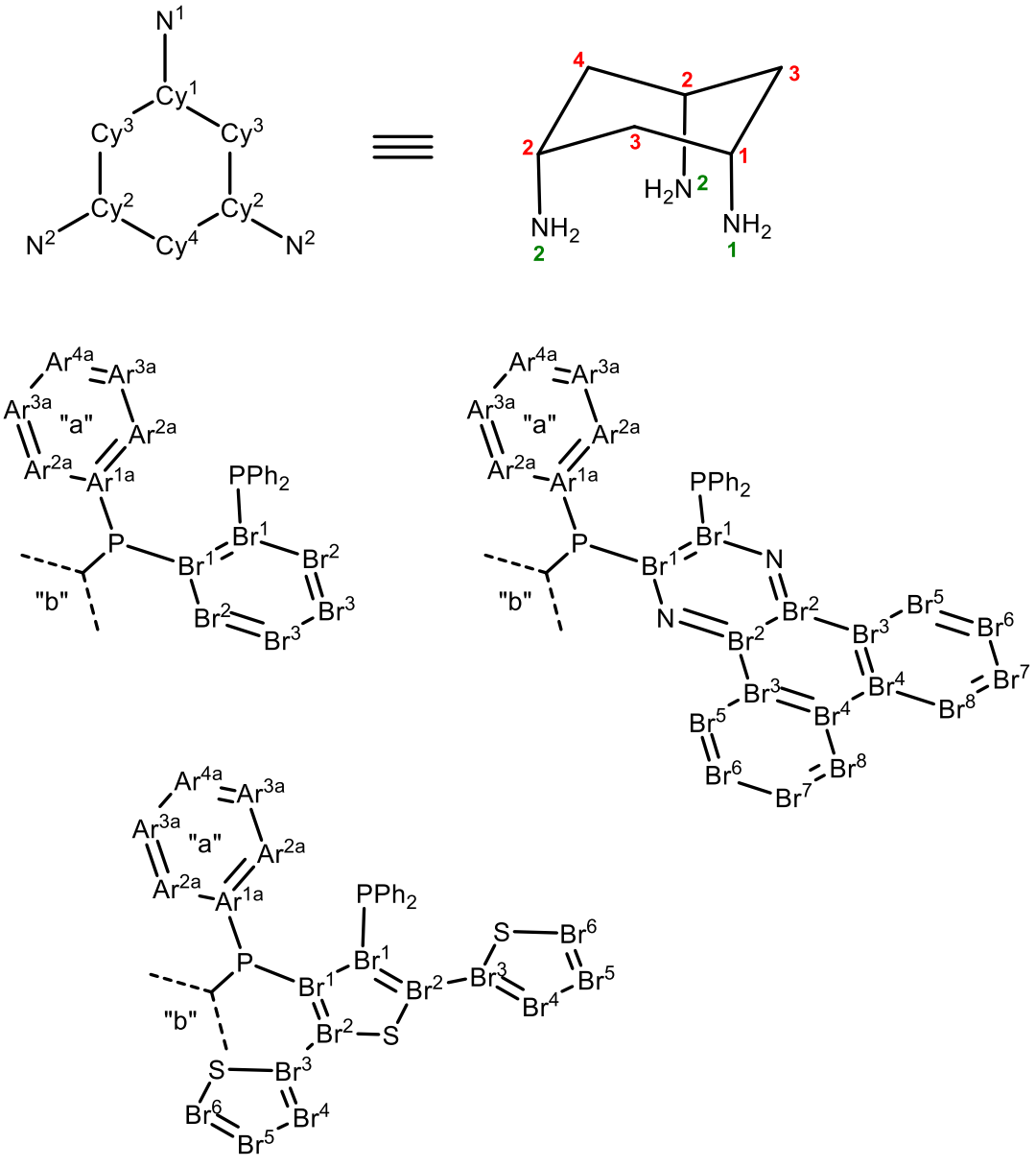

Synthesis of [RuCl(dmso-*S*)$_2$(κ^3-tach)]Cl, 1

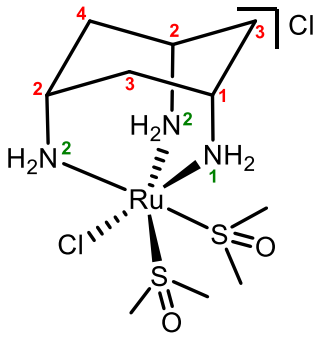

Following the literature procedure.[7] *cis-cis*-1,3,5-triaminocyclohexane (0.330 g, 2.55 mmol) was added to a solution of [$RuCl_2$(dmso-*S*)$_3$(dmso-*O*)] (1.24 g, 2.55 mmol) in dimethylsulfoxide (100 mL). The mixture was heated to 130 °C for 1 h yielding a yellow solution before being cooled and the complex precipitated from ethyl acetate (1000 mL). The mixture was cooled to –20 °C for 18 h forming more precipitate. The precipitate was collected by filtration, washed with ethyl acetate (200 mL) and dried *in vacuo* to give **1** as a pale yellow solid. Yield: 795 mg (74%).

^{1}H NMR (400 MHz, D_2O) (*δ*, ppm): 4.50 (d, $^2J_{HH}$ = 12.2 Hz, 2H, N*H*$_2$, N^2), 4.21 (d, $^2J_{HH}$ = 12.2 Hz, 2H, N*H*$_2$, N^2), 3.86 (s, 2H, N*H*$_2$, N^1), 3.50 (s, 2H, C*H*, Cy^2), 3.33 (s, 12H, (C*H*$_3$)SO), 3.23 (s, 1H, C*H*, Cy^1), 2.19–1.94 (m, 4H, C*H*$_2$, Cy^3 + Cy^4), 1.81 (d, $^2J_{HH}$ = 15.2 Hz, 2H, C*H*$_2$, Cy^3).

^{13}C{^{1}H} NMR (101 MHz, D_2O) (*δ*, ppm): 44.5 (s, (*C*H$_3$)$_2$SO), 43.9 (s, *C*H, Cy^1), 42.8 (s, *C*H, Cy^2), 33.0 (s, *C*H$_2$, Cy^4), 32.1 (s, *C*H$_2$, Cy^3).

HRMS (ESI): *m/z* calculated for $C_{10}H_{27}ClN_3O_2RuS_2$ $[M]^{\bullet+}$ = 422.0269, found = 422.0263.

Synthesis of 3',4'-bis(diphenylphosphanyl)-2,2':5',2''-terthiophene, L1

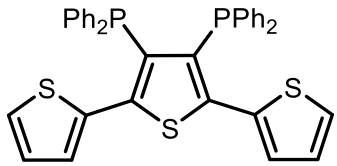

A solution of 3',4'-dibromo-2,2':5',2''-terthiophene (914 mg, 2.25 mmol) in Et_2O (30 mL) was cooled to –78 °C and a solution of n-butyllithium (1.6 M in hexane) (1.55 mL, 2.48 mmol) was added dropwise. A yellow precipitate was observed, and the solution was stirred at –78 °C for 2 h before chlorodiphenylphosphine (0.41 mL, 2.25 mmol) was added. The mixture was slowly warmed to room temperature and stirred for 18 h. The mixture was filtered to remove the lithium chloride precipitate and the solvent removed *in vacuo* to give the monophosphine intermediate as a yellow powder. The procedure was repeated to give the diphosphine. The residue was purified by a short silica plug (eluting Et_2O/CH_2Cl_2) to obtain pure **4** as a yellow solid. Yield: 0.275 g (20%).

^{1}H NMR (400 MHz, $CDCl_3$) (δ, ppm): 7.25 – 7.19 (m, 8H, P*Ph*$_2$), 7.12 – 7.09 (m, 12H, P*Ph*$_2$), 7.07 (dd, $^3J_{HH}$ = 5.1 Hz, $^4J_{HH}$ = 1.3 Hz, 2H, C*H*), 6.63 (dd, $^3J_{HH}$ = 5.1 Hz, $^4J_{HH}$ = 3.6 Hz, 2H, C*H*), 6.60 (dd, $^3J_{HH}$ = 3.6, $^4J_{HH}$ = 1.2 Hz, 2H, C*H*).

^{13}C{^{1}H} NMR (101 MHz, $CDCl_3$) (δ, ppm): 144.0, 139.3, 135.5, 134.1, 132.5, 129.4, 127.9, 127.7, 127.2, 126.9.

^{31}P{^{1}H} NMR (162 MHz, $CDCl_3$) (δ, ppm): –17.3 (s, 2P).

HRMS (MALDI): *m/z* calculated for $C_{36}H_{26}P_2S_3$ $[M+H]^{\bullet+}$ = 617.0745, found = 617.0752.

Synthesis of 2,3-dichlorodibenzo[f,h]quinoxaline

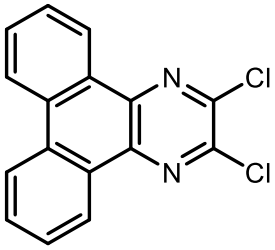

1,4-dihydrodibenzo[f,h]quinoxaline-2,3-dione (0.600 g, 2.30 mmol), PCl_3 (4.0 mL, 46.0 mmol) and DMF (9 mL) were heated to 100 °C for 16 h. The dark red solution was cooled to room temperature and the product precipitated by the addition of degassed water. The yellow solid was collected by filtration, washed with ethanol and dried *in vacuo*. Yield: 0.75 g (84%).

^{1}H NMR (400 MHz, $CDCl_3$) (δ, ppm): 9.07 (d, $^{3}J_{HH}$ = 7.5 Hz, 2H, C*H*), 8.63 (d, $^{3}J_{HH}$ = 8.2 Hz, 2H, C*H*), 7.83 (t, $^{3}J_{HH}$ = 7.2 Hz, 2H, C*H*), 7.75 (t, $^{3}J_{HH}$ = 7.5 Hz, 2H, C*H*).

^{13}C{^{1}H} NMR (100 MHz, $CDCl_3$) (δ, ppm): 139.6, 137.3, 131.9, 130.4, 128.2, 126.0, 126.0, 123.0.

HRMS (APCI): *m/z* calculated for $C_{16}H_8N_2Cl_2$ $[M]^{\bullet+}$ = 299.0137, found = 299.0130. *APCI mass spectrum exhibited the expected chlorine isotope pattern.*

Synthesis of 2,3-bis(diphenylphosphino)dibenzo[f,h]quinoxaline, L3

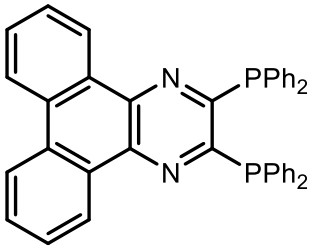

A solution of diphenylphosphine (0.35 mL, 2.0 mmol) in THF (10 mL) was cooled to –78 °C and a solution of n-butyllithium (1.6 M in hexane, 1.38 mL, 2.2 mmol) was added dropwise. The orange solution was stirred at this temperature for 2 h before a solution of 2,3-dichlorodibenzo[f,h]quinoxaline (270 mg, 0.90 mmol) in THF (5 mL) was added dropwise and stirred for a further 12 h with warming to room temperature. The solution was quenched at –78 °C by the addition of sat. aq. NH_4Cl (5 mL) and warmed to room temperature. The aqueous layer was extracted with THF (3 x 10 mL) and filtered through silica. The volatiles were removed *in vacuo*, the residue dissolved in EtOAc and filtered to remove soluble impurities. The remaining solid was recrystallised from EtOAc to give a yellow solid. Yield: 0.12 g (22%).

^{1}H NMR (400 MHz, $CDCl_3$) (δ, ppm): 8.67 (dd, $^{3}J_{HH}$ = 8.0 Hz, $^{4}J_{HH}$ = 1.4 Hz, 2H, C*H*), 8.57 – 8.53 (m, 2H, C*H*), 7.72 (ddd, $^{3}J_{HH}$ = 8.4 Hz, $^{3}J_{HH}$ = 7.0 Hz, $^{4}J_{HH}$ = 1.5 Hz, 2H, C*H*), 7.56 (ddd, $^{3}J_{HH}$ = 8.1 Hz, $^{3}J_{HH}$ = 7.0 Hz, $^{4}J_{HH}$ = 1.2 Hz, 2H, C*H*), 7.44 – 7.36 (m, 8H, P*Ph*$_2$), 7.34 – 7.25 (m, 12H, P*Ph*$_2$).

^{13}C{^{1}H} NMR (100 MHz, $CDCl_3$) (δ, ppm): 162.3 – 162.0 (m), 140.2, 136.1, 134.8, 131.7, 130.1, 129.7, 128.9, 128.3, 127.8, 125.8, 122.7.

^{31}P{^{1}H} NMR (162 MHz, $CDCl_3$) (δ, ppm): –10.24 (s, 2P).

HRMS (ESI): *m/z* calculated for $C_{40}H_{29}N_2P_2$ $[M+H]^{\bullet+}$ = 599.1800, found = 599.1809.

Synthesis of [RuCl(dppbz)(κ^3-tach)]Cl, 3f

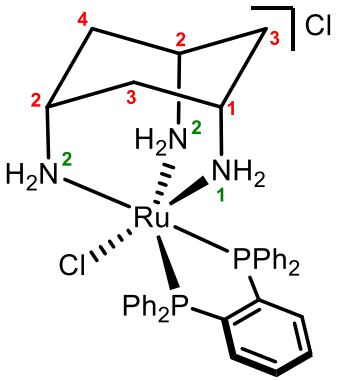

A solution of **1** (50 mg, 0.11 mmol) and 1,2-bis(diphenylphosphine)benzene (80 mg, 0.18 mmol, 1.8 eq) in anhydrous methanol (15 mL) was heated to reflux for 48 h. The solution was cooled, unreacted phosphine was removed by filtration and the solution was concentrated (approx. 5 mL). Diethyl ether (90 mL) was added to precipitate the product which was collected by filtration and dried to give a pale yellow solid. Yield: 62 mg (77%).

^{1}H NMR (500 MHz, CD_3OD) (δ, ppm): 8.07 (ddd, $^3J_{HP}$ = 9.8 Hz, $^3J_{HH}$ = 5.4 Hz, $^4J_{HH}$ = 1.9 Hz, 4H, P*Ph*$_2$, Ar^{2a}), 7.55 – 7.49 (m, 6H: 2H, P*Ph*$_2$, Ar^{4a}; 4H, PC$_6$*H*$_4$P, Br^2 + Br^3), 7.45 (t, $^3J_{HH}$ = 7.7 Hz, 4H, P*Ph*$_2$, Ar^{3a}), 7.41 – 7.37 (m, 4H, P*Ph*$_2$, Ar^{3b}), 7.37 – 7.32 (m, 2H, P*Ph*$_2$, Ar^{4b}), 7.15 (ddd, $^3J_{HP}$ = 9.5 Hz, $^3J_{HH}$ = 5.9 Hz, $^4J_{HH}$ = 1.6 Hz, 4H, P*Ph*$_2$, Ar^{2b}), 4.92 (d, $^2J_{HH}$ = 12.1 Hz, 2H, N*H*$_2$, N^2), 3.86 (d, $^2J_{HH}$ = 12.0 Hz, 2H, N*H*$_2$, N^2), 3.56 (s, 2H, C*H*, Cy^2), 2.72 (s, 1H, C*H*, Cy^1), 2.29 (d, $^2J_{HH}$ = 15.1 Hz, 1H, C*H*$_2$, Cy^4), 2.14 (d, $^2J_{HH}$ = 15.3 Hz, 1H, C*H*$_2$, Cy^4), 1.86 (d, $^2J_{HH}$ = 15.0 Hz, 2H, C*H*$_2$, Cy^3), 1.74 (d, $^2J_{HH}$ = 15.9 Hz, 2H, C*H*$_2$, Cy^3), 1.39 (s, 2H, N*H*$_2$, N^1).

^{13}C{^{1}H} NMR (126 MHz, CD_3OD) (δ, ppm): 145.6 (vt, $|^1J_{PC} + {}^2J_{P'C}|$ = 82 Hz, PC$_6$H$_4$P, Br^1), 136.8 (t, $|^2J_{PC} + {}^4J_{P'C}|$ = 10 Hz, P*Ph*$_2$, Ar^{2a}), 133.6 (m P*Ph*$_2$, Ar^{1a} + Ar^{1b}), 133.5 (t, $|^2J_{PC} + {}^3J_{P'C}|$ = 16 Hz, PC$_6$H$_4$P, Br^2), 133.0 (t, $|^3J_{PC} + {}^4J_{P'C}|$ = 9 Hz, P*Ph*$_2$, Ar^{2b}), 131.8 (s, PC$_6$H$_4$P, Br^3), 131.7 (s, P*Ph*$_2$, Ar^{4a}), 131.1 (s, P*Ph*$_2$, Ar^{4b}), 130.5 (t, $|^3J_{PC} + {}^5J_{P'C}|$ = 9 Hz, P*Ph*$_2$, Ar^{3b}), 129.5 (t, $|^3J_{PC} + {}^5J_{P'C}|$ = 9 Hz, P*Ph*$_2$, Ar^{3a}), 44.8 (s, *C*H, Cy^2), 44.4 (s, *C*H, Cy^1), 35.6 (s, *C*H$_2$, Cy^4), 34.3 (s, *C*H$_2$, Cy^3).

^{31}P{^{1}H} NMR (162 MHz, CD_3OD) (δ, ppm): 73.0 (s, 2P).

Elemental analysis for [RuCl(dppbenz)(*cis*-tach)]Cl.CH_2Cl_2 ($C_{37}H_{41}Cl_4N_3P_2Ru$): calcd. C, 53.38; H, 4.96; N, 5.05%. Found: C, 53.61; H, 4.84; N, 5.14%.

HRMS (ESI): *m/z* calculated for $C_{36}H_{39}ClN_3P_2RuS_3$ $[M]^{\bullet+}$ = 712.1352, found = 712.1357. *ESI mass spectrum exhibited the expected ruthenium/chlorine isotope pattern for **3f**.*

Synthesis of [RuCl(L1)(κ^3-tach)]Cl, 3g

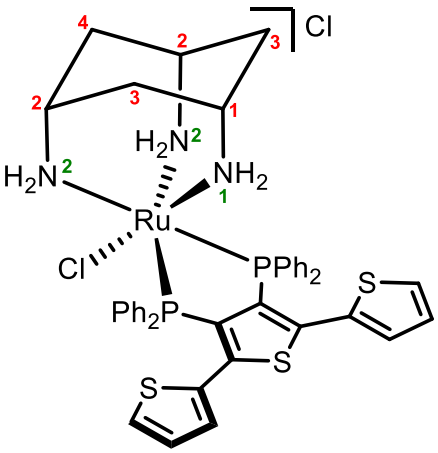

A solution of **1** (27 mg, 0.060 mmol) and **L1** (67 mg, 0.11 mmol, 1.8 eq) in anhydrous methanol (15 mL) was heated to reflux for 18 h. The solution was cooled, unreacted phosphine was removed by filtration and the solvent was removed *in vacuo*. The residue was dissolved in dichloromethane (1 mL), and diethyl ether (15 mL) was added to precipitate the product which was collected by filtration and dried to give a pale yellow solid. Yield: 36 mg (65%).

^{1}H NMR (500 MHz, CD_2Cl_2) (δ, ppm): 7.81 – 7.76 (m, 4H, P*Ph*$_2$, Ar^{2a}), 7.67 – 7.59 (m, 4H, P*Ph*$_2$, Ar^{2b}), 7.54 (t, $^3J_{HH}$ = 7.7 Hz, 4H, P*Ph*$_2$, Ar^{3a}), 7.42 (t, $^3J_{HH}$ = 7.4 Hz, 4H, P*Ph*$_2$, Ar^{4a}), 7.18 (t, $^3J_{HH}$ = 7.4 Hz, 2H, P*Ph*$_2$, Ar^{4b}), 7.08 (dd, $^3J_{HP}$ = 15.5 Hz, $^3J_{HH}$ = 6.9 Hz, 4H, P*Ph*$_2$, Ar^{3b}), 7.04 (dd, $^3J_{HH}$ = 5.1 Hz, $^4J_{HH}$ = 1.2 Hz, 2H, C*H*, Br^6), 6.51 (dd, $^3J_{HH}$ = 5.1 Hz, $^4J_{HH}$ = 3.6 Hz, 2H, C*H*, Br^5), 6.39 (dd, $^3J_{HH}$ = 3.6 Hz, $^4J_{HH}$ = 1.2 Hz, 2H, C*H*, Br^4), 4.21 (d, $^2J_{HH}$ = 12.0 Hz, 2H, N*H*$_2$, N^2), 3.58 (s, 2H, C*H*, Cy^2), 3.21 (d, $^2J_{HH}$ = 12.0 Hz, 2H, N*H*$_2$, N^2), 2.80 (s, 1H, C*H*, Cy^1), 2.07 – 1.89 (m, 4H; 2H, C*H*$_2$, Cy^3, 2H, C*H*$_2$, Cy^4), 1.81 (d, $^2J_{HH}$ = 15.8 Hz, 2H, C*H*$_2$, Cy^3), 1.46 (s, 2H, N*H*$_2$, N^1).

^{13}C{^{1}H} NMR (126 MHz, CD_2Cl_2) (δ, ppm): 143.9 (vt, $|^1J_{PC} + {}^2J_{P'C}|$ = 84 Hz, P*C*$_{12}$S$_3$P, Br^1), 134.7 (t, $|^2J_{PC} + {}^4J_{P'C}|$ = 10 Hz, P*Ph*$_2$, Ar^{2a}), 132.5 (t, $|^2J_{PC} + {}^4J_{P'C}|$ = 10 Hz, P*Ph*$_2$, Ar^{2b}), 132.3 (s, P*C*$_{12}$S$_3$P, Br^2), 130.7 (s, P*Ph*$_2$, Ar^{4a} + Ar^{4b}), 130.3 (s, P*Ph*$_2$, Ar^{3a}), 130.2 – 130.0 (m, P*C*$_{12}$S$_3$P, Br^4 + Br^3, Ar^{1a} + Ar^{1b}), 128.3 (s, P*C*$_{12}$S$_3$P, Br^6), 128.1 (t, $|^3J_{PC} + {}^5J_{P'C}|$ = 10 Hz, P*Ph*$_2$, Ar^{3b}), 127.7 (s, P*C*$_{12}$S$_3$P, Br^5), 43.7 (s, *C*H, Cy^1), 43.6 (s, *C*H, Cy^2), 35.4 (s, *C*H$_2$, Cy^4), 34.2 (s, *C*H$_2$, Cy^3).

^{31}P{^{1}H} NMR (162 MHz, CD_2Cl_2) (δ, ppm): 56.2 (s, 2P).

Elemental analysis for [RuCl(**L1**)(*cis*-tach)]Cl.CH_2Cl_2 ($C_{43}H_{43}Cl_4N_3P_2RuS_3$): calcd. C, 51.50; H, 4.32; N, 4.19%. Found: C, 51.52; H, 4.40; N, 4.20%.

HRMS (ESI): *m/z* calculated for $C_{42}H_{41}ClN_3P_2RuS_3$ $[M]^{\bullet+}$ = 882.0671, found = 882.0685. *ESI mass spectrum exhibited the expected ruthenium/chlorine isotope pattern for **3g**.*

Synthesis of [RuCl(L2)(κ³-tach)]Cl, 3h

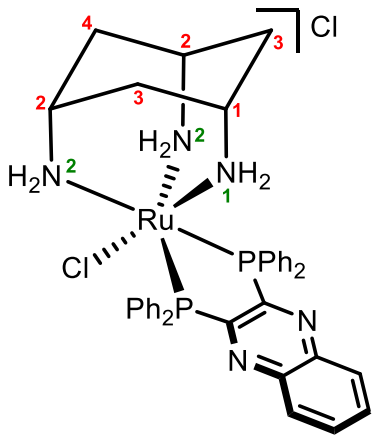

A solution of **1** (27 mg, 0.060 mmol) and **L2** (54 mg, 0.11 mmol, 1.8 eq) in anhydrous methanol (15 mL) was heated to reflux for 48 h. The solution was cooled, unreacted phosphine was removed by filtration and the solvent was removed *in vacuo*. The residue was dissolved in dichloromethane (1 mL), and diethyl ether (15 mL) was added to precipitate the product which was collected by filtration and dried to give a red solid. Yield: 21 mg (44%).

^{1}H NMR (500 MHz, CD_3OD) (δ, ppm): 8.19 (ddd, $^{3}J_{HP}$ = 7.9 Hz, $^{3}J_{HH}$ = 7.1 Hz, $^{4}J_{HH}$ = 3.3 Hz, 4H, P*Ph*$_2$, Ar^{2a}), 8.08 (dd, $^{3}J_{HH}$ = 6.5 Hz, $^{4}J_{HH}$ = 3.5 Hz, 2H, C*H*, Br^{3}), 7.93 (dd, $^{3}J_{HH}$ = 6.5 Hz, $^{4}J_{HH}$ = 3.5 Hz, 2H, C*H*, Br^{4}), 7.52 (t, $^{3}J_{HH}$ = 7.2 Hz, 4H, P*Ph*$_2$, Ar^{4a}), 7.45 (t, $^{3}J_{HH}$ = 7.0 Hz, 4H, P*Ph*$_2$, Ar^{3a}), 7.38 – 7.34 (m, 6H, P*Ph*$_2$, Ar^{3b} + Ar^{4b}), 7.14 (ddd, $^{3}J_{HP}$ = 7.9 Hz, $^{3}J_{HH}$ = 7.2 Hz, $^{4}J_{HH}$ = 3.3 Hz, 4H, P*Ph*$_2$, Ar^{2b}), 5.10 (d, $^{2}J_{HH}$ = 12.0 Hz, 2H, N*H*$_2$, N^{2}), 4.15 (d, $^{2}J_{HH}$ = 11.9 Hz, 2H, N*H*$_2$, N^{2}), 3.62 (s, 2H, C*H*, Cy^{2}), 2.78 (s, 1H, C*H*, Cy^{1}), 2.40 (d, $^{2}J_{HH}$ = 15.0 Hz, 1H, C*H*$_2$, Cy^{4}), 2.18 (d, $^{2}J_{HH}$ = 15.0 Hz, 1H, C*H*$_2$, Cy^{4}), 1.90 (d, $^{2}J_{HH}$ = 15.6 Hz, 2H, C*H*$_2$, Cy^{3}), 1.76 (d, $^{2}J_{HH}$ = 15.3 Hz, 2H, C*H*$_2$, Cy^{3}), 1.58 (s, 2H, N*H*$_2$, N^{1}).

^{13}C{^{1}H} NMR (126 MHz, CD_3OD) (δ, ppm): 159.9 (vt, $|^{1}J_{PC} + {}^{2}J_{P'C}|$ = 111 Hz, P*C*$_8$N$_2$P, Br^{1}), 138.1 (t, $|^{2}J_{PC} + {}^{4}J_{P'C}|$ = 10 Hz, P*Ph*$_2$, Ar^{2a}), 133.7 (s, P*C*$_8$N$_2$P, Br^{4}), 132.9 (t, $|^{2}J_{PC} + {}^{4}J_{P'C}|$ = 10 Hz, P*Ph*$_2$, Ar^{2b}), 131.9 (s, P*Ph*$_2$, Ar^{4a} + Ar^{4b}), 131.2 (s, P*C*$_8$N$_2$P, Br^{2}), 131.1 (s, P*C*$_8$N$_2$P, Br^{3}), 130.6 (t, $|^{3}J_{PC} + {}^{5}J_{P'C}|$ = 9 Hz, P*Ph*$_2$, Ar^{3a}), 128.9 (t, $|^{3}J_{PC} + {}^{5}J_{P'C}|$ = 9 Hz, P*Ph*$_2$, Ar^{3b}), 44.8 (s, *C*H, Cy^{2}), 44.4 (s, *C*H, Cy^{1}), 35.5 (s, *C*H$_2$, Cy^{4}), 34.3 (s, *C*H$_2$, Cy^{3}).

^{31}P{^{1}H} NMR (162 MHz, CD_3OD) (δ, ppm): 63.9 (s, 2P).

Elemental analysis for [RuCl(**L2**)(*cis*-tach)]Cl.CH_2Cl_2 ($C_{39}H_{41}Cl_4N_3P_2Ru$): calcd. C, 52.95; H, 4.67; N, 7.92%. Found: C, 52.69; H, 4.69; N, 7.71%.

HRMS (ESI): *m/z* calculated for $C_{38}H_{39}ClN_5P_2Ru$ $[M]^{\bullet+}$ = 764.1414, found = 764.1411. *ESI mass spectrum exhibited the expected ruthenium/chlorine isotope pattern for* ***3h***.

Synthesis of [RuCl(L3)(κ^3-tach)]Cl, 3i

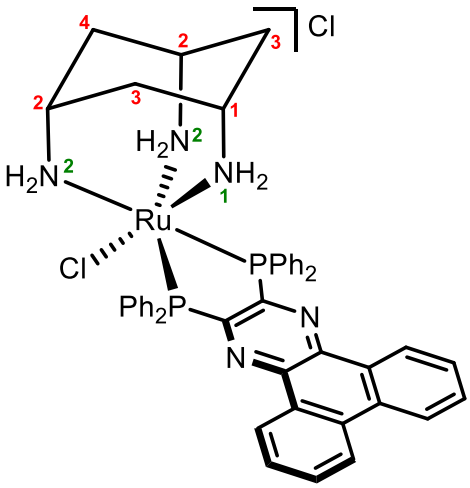

A solution of **1** (32 mg, 0.070 mmol) and **L3** (54 mg, 0.091 mmol, 1.3 eq) in anhydrous ethanol (20 mL) was heated to reflux for 48 h. The solution was cooled, unreacted phosphine was removed by filtration and the solvent was removed *in vacuo*. The residue was dissolved in dichloromethane (1 mL), and diethyl ether (15 mL) was added to precipitate the product which was collected by filtration and dried to give a red solid. Yield: 25 mg (40%).

^{1}H NMR (500 MHz, CD_3OD) (δ, ppm): 8.49 – 8.42 (m, 6H; 4H, P*Ph*$_2$, Ar^{2a}, 2H, C*H*, Br^6), 7.78 (d, $^3J_{HH}$ = 7.8 Hz, 2H, C*H*, Br^5), 7.68 (t, $^3J_{HH}$ = 7.1 Hz, 2H, P*Ph*$_2$, Ar^{3b}), 7.63 (t, $^3J_{HH}$ = 7.4 Hz, 4H, P*Ph*$_2$, Ar^{4a} + Ar^{4b}), 7.34 – 7.26 (m, 6H; 4H, P*Ph*$_2$, Ar^{3a}, 2H, P*Ph*$_2$, Ar^{3b}), 7.21 – 7.12 (m, 8H; 4H, P*Ph*$_2$, Ar^{2b}, 2H, C*H*, Br^7, 2H, C*H*, Br^8), 5.33 (d, $^2J_{HH}$ = 11.8 Hz, 2H, N*H*$_2$, N^2), 4.27 (d, $^2J_{HH}$ = 11.8 Hz, 2H, N*H*$_2$, N^2), 3.69 (s, 2H, C*H*, Cy^2), 2.72 (s, 1H, C*H*, Cy^1), 2.48 (d, $^2J_{HH}$ = 15.0 Hz, 1H, C*H*$_2$, Cy^4), 2.24 (d, $^2J_{HH}$ = 15.0 Hz, 1H, C*H*$_2$, Cy^4), 1.91 (d, $^2J_{HH}$ = 15.5 Hz, 2H, C*H*$_2$, Cy^3), 1.74 (d, $^2J_{HH}$ = 15.4 Hz, 2H, C*H*$_2$, Cy^3), 1.45 (s, 2H, N*H*$_2$, N^1).

^{13}C{^{1}H} NMR (126 MHz, CD_3OD) (δ, ppm): 158.8 (vt, $|^1J_{PC} + {}^2J_{P'C}|$ = 112 Hz, P*C*$_4$N$_2$P, Br^1), 141.3 (s, P*C*$_{16}$N$_2$P, Br^3), 138.7 ($|^2J_{PC} + {}^4J_{P'C}|$ = 10 Hz, P*Ph*$_2$, Ar^{2a}), 133.1 (m P*Ph*$_2$, Ar^{1a} + Ar^{1b}), 132.9 (t, $|^2J_{PC} + {}^4J_{P'C}|$ = 10 Hz, P*Ph*$_2$, Ar^{2b}), 132.1 (s, P*C*$_{16}$N$_2$P, Br^8), 132.0 (s, P*Ph*$_2$, Ar^{4a} + Ar^{4b}), 131.1 (s, P*C*$_{16}$N$_2$P, Br^2), 130.5 (t, $|^3J_{PC} + {}^5J_{P'C}|$ = 9 Hz, P*Ph*$_2$, Ar^{3a}), 129.6 (s, P*C*$_{16}$N$_2$P, Br^4), 128.9 (t, $|^3J_{PC} + {}^5J_{P'C}|$ = 9 Hz, P*Ph*$_2$, Ar^{3b}), 128.5 (s, P*C*$_{16}$N$_2$P, Br^7), 126.5 (s, P*C*$_{16}$N$_2$P, Br^6), 123.4 (s, P*C*$_{16}$N$_2$P, Br^5), 44.8 (s, *C*H, Cy^2), 44.4 (s, *C*H, Cy^1), 35.7 (s, *C*H$_2$, Cy^4), 34.3 (s, *C*H$_2$, Cy^3).

^{31}P{^{1}H} NMR (162 MHz, CD_3OD) (δ, ppm): 63.3 (s, 2P).

Elemental analysis for [RuCl(**L3**)(*cis*-tach)]Cl.1.5CH_2Cl_2 ($C_{47.5}H_{46}Cl_5N_5P_2Ru$): calcd. C, 55.54; H, 4.51; N, 6.82%. Found: C, 55.54; H, 4.78; N, 7.17%.

HRMS (ESI): *m/z* calculated for $C_{46}H_{43}ClN_5P_2Ru$ $[M]^{\bullet+}$ = 864.1726, found = 864.1710. *ESI mass spectrum exhibited the expected ruthenium/chlorine isotope pattern for **3i**.*

Kinetics of Aquation

Sodium phosphate solutions were prepared prior to addition of ruthenium complex. Solutions were stored in the dark in a sealed vessel prior to use. A stock solution of **3b**, **3f** or **3h** (50 µL, 20 mM) in CD_3OD was added to a sodium phosphate solution (3 mL, pH 7.4) giving a final concentration of approx. 300 µM. The absorbance was recorded at 5 intervals at T = 288–310 K. After the reaction was complete (no change in absorbance was observed), the ^{1}H NMR spectrum was recorded using a Bruker Avance AV500 spectrometer at the required temperature (288–310 K) using solvent suppression techniques and CD_3OD as deuterium lock.

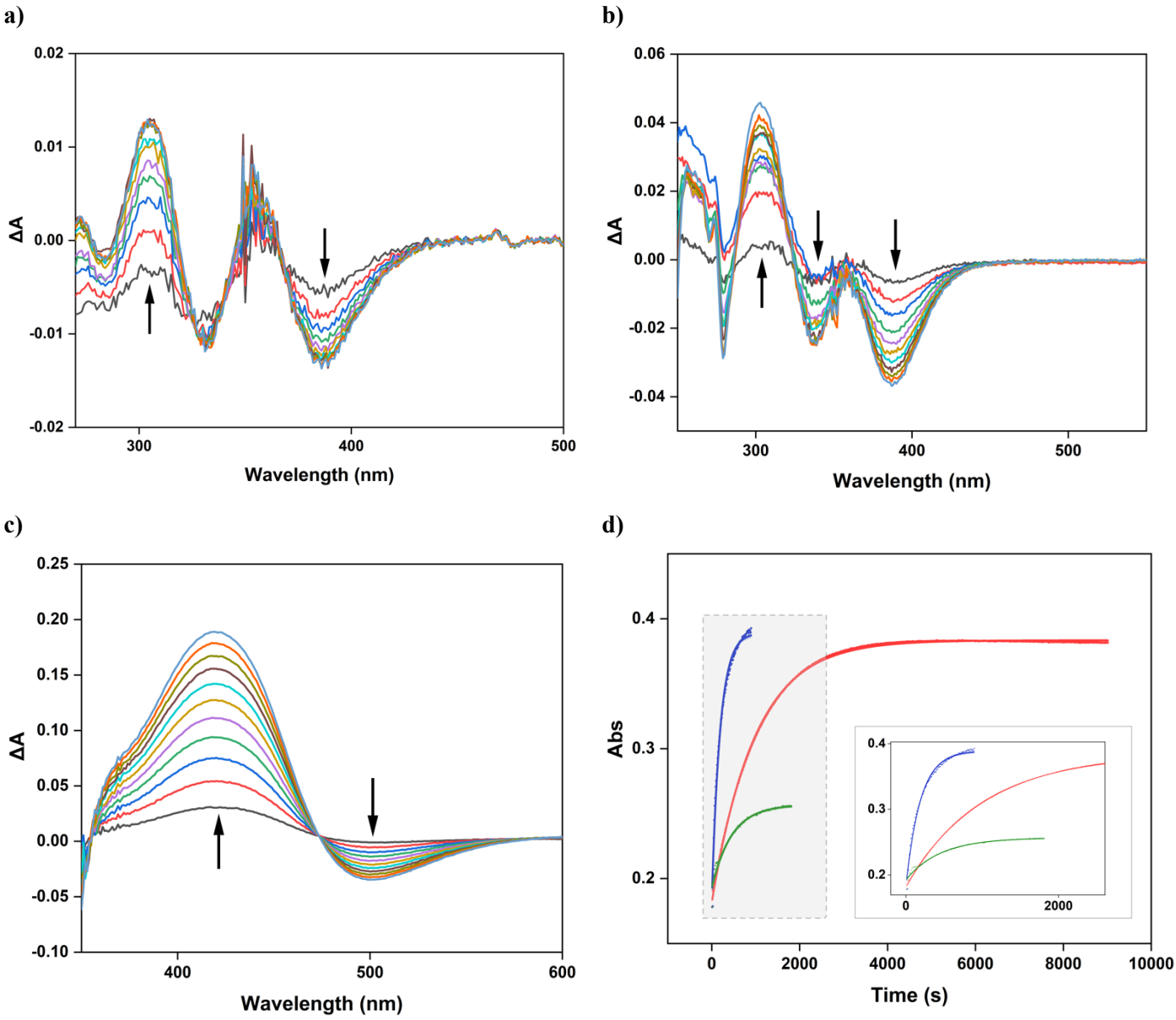

Figure S1. Time-evolution of UV/Vis difference spectra for the aquation of 300 µM of a) **3b**, b) **3f**, c) **3h** in aqueous solution buffered at pH 7.4 (10 mM sodium phosphate) with 1.6% MeOD at 298 K, $I \approx 25$ mM. Plots are given for minutes 1 to 9. $\Delta A = A_t - A_0$, where A_t = absorbance at time t and $A_0 = A$ at t = 30 s. d) Time dependence of the absorbance (green **3b**, blue **3f**, red **3h**) indicated (up arrow) for each complex, inset is an expansion to show the first 2000 s.

Determination of the pK_a of the Ru–OH_2

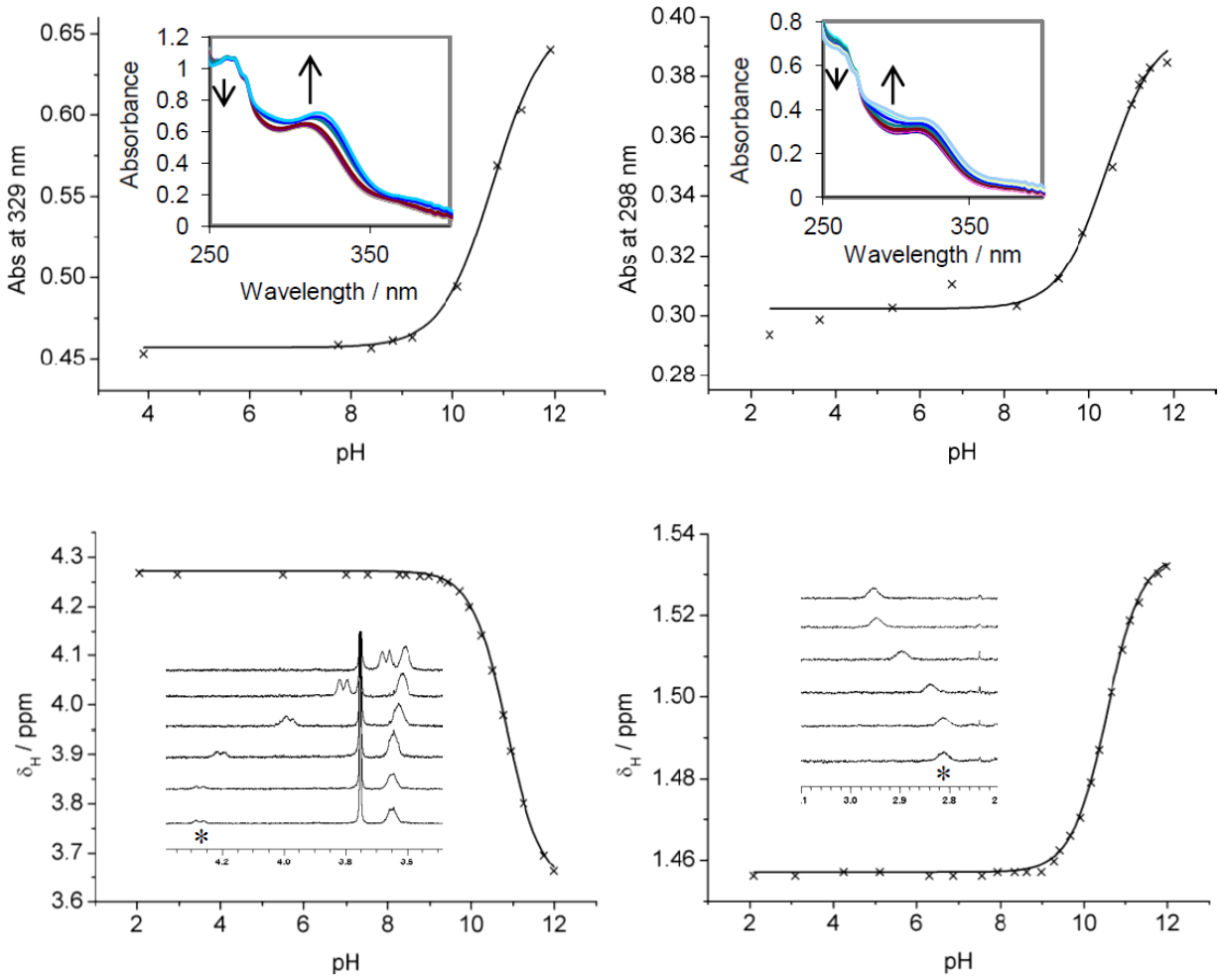

Figure S2. Determination of pK_a of coordinated aqua ligand of **3b** (left) and **3c** (right) by UV/Visible (top) and ^{1}H NMR (bottom) titrations. * indicates one of three selected ^{1}H resonances for **3b** (NH_2, pK_a 10.85 ± 0.01) and **3c** (CH, pK_a 10.53 ± 0.01). The inset shows the shift of the resonance during the experiment.

Equilibrium of Aquation/Anation

Equilibrium constants were calculated in the kinetic analyses, however, these were not obtained under physiologically-relevant conditions due to the difference in ionic strength of the solution; a relevant ionic strength, *I*, is of the order of 10^{-1} M. Rearrangement of the equilibrium equation, $\frac{[chlorido]}{[aqua]} = \frac{[Cl^-]}{K}$ permits the calculation of *K* by variation of chloride concentration and the determination of the concentrations of the ruthenium species present in the solution.

Aqueous solutions of the appropriate complex (500 μM) and sodium chloride (0 to 100 mM) at pH 7.4 (10 mM sodium phosphate) with 1.6% CD_3OD were heated at 37°C for 2 h before the ^1H (**3b**) or ^1H and $^{31}P\{^1H\}$ (**3c**) NMR spectra were recorded at 37 °C. Deprotonation of the aqua ligand is not expected to occur at pH 7.4 and therefore to not affect any speciation observed. Relative integrations of the chlorido and aqua species were calculated for each chloride concentration, the plots of which are given in Figure S3. The ruthenium-phosphate adduct, although present, was not accounted for in the analysis.

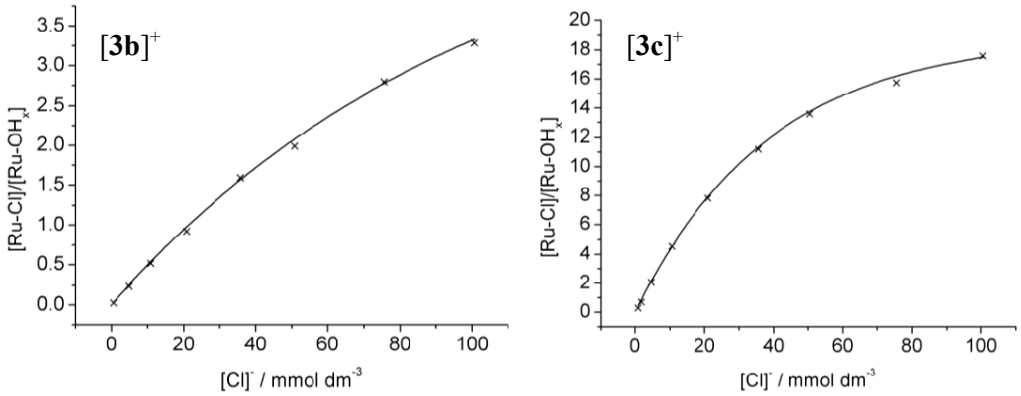

Figure S3. Plots of the fraction of chlorido/aquated species and $[Cl^-]$ for $[\mathbf{3b}]^+$ (left) and $[\mathbf{3c}]^+$ (right) vs. chloride concentration at pH 7.4 (10 mM sodium phosphate) and 37°C.

The equilibrium constant *K* was calculated from the fitted curve for the aquation of each complex at an ionic strength of approximately 130 mM, corresponding to 104 mM sodium chloride and 10 mM sodium phosphate at pH 7.4. In order to illustrate the physiological relevance of the equilibrium constant, the predicted distribution of chlorido and aqua species are given in Table S1 for the blood, cytoplasm and cell nucleus.[8,9]

Table S1. Equilibrium constants and proportion of ruthenium species aquated under various physiologically relevant conditions.

			Predicted % Aqua[a] (Ru–OH_2) at pH 7.4		
	K (10^{-3} M)	pK_a[b]	Blood[c]	Cytoplasm[d]	Nucleus[e]
3b	30.6 ± 1.7[f]	10.85 ± 0.02	22.8 ± 1.2	48.6 ± 3.2	88.5 ± 4.9
3c	5.90 ± 0.08[f]	10.54 ± 0.02	5.4 ± 0.1	20.7 ± 0.3	59.6 ± 0.8
RM175[g 8]	9.1 ± 0.9[h]	7.71 ± 0.01	5.2[i]	18.6[i]	45.2[i]
HC11[j 8]	11.7 ± 0.7[h]	8.01 ± 0.03	8.8[i]	29.7[i]	65.2[i]
RAPTA-C[10]	3.8 ± 0.2[k]	9.2[i,l]	[m]	[m]	[m]
$[PtCl_2(en)]$[11]	[n]	6.53[i]	2.7[i]	[m]	42.0[i]

a) predicted, based on K, b) T = 298 K, values given for first aqua deprotonation only (if applicable), c) 104 mM, d) 22.7 mM, e) 4 mM NaCl, f) T = 310 K, I = 130 mM, g) $[RuCl(\eta^6\text{-bip})(en)]PF_6$, h) T = 310 K, I = 100 mM, i) No standard deviations reported; remainder of species made up of both chlorido and hydroxy species, j) $[RuCl(\eta^6\text{-tha})(en)]PF_6$, k) T = 298 K, I = 150 mM, l) Calculated pK_a for $[RuCl(OH_2)(\eta_6\text{-}C_6H_6)(PTA)]^+$, m) no speciation reported, n) 296 K, I = 200 mM.

Interactions with Nucleosides

To evaluate the potential for **3b** to form covalent bonds to the N7 of a guanine residue, the complex was heated at 310 K for 24 h with one equivalent of EtG or GMP (1 mM) in H_2O. The solutions were characterised by ^{1}H and $^{31}P\{^{1}H\}$ NMR spectroscopy, supplemented with 1.6% CD_3OD as a lock solvent.

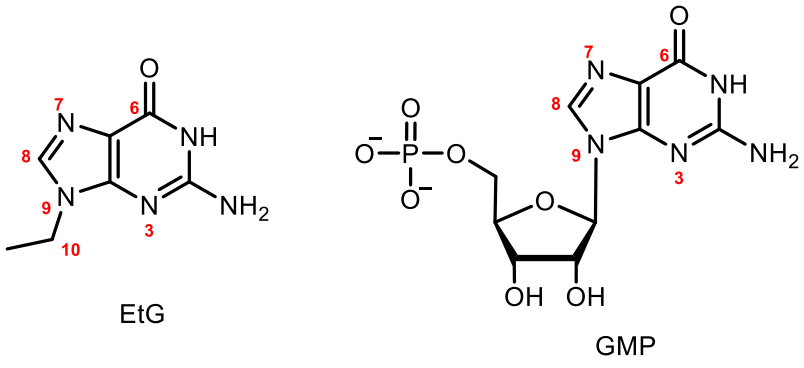

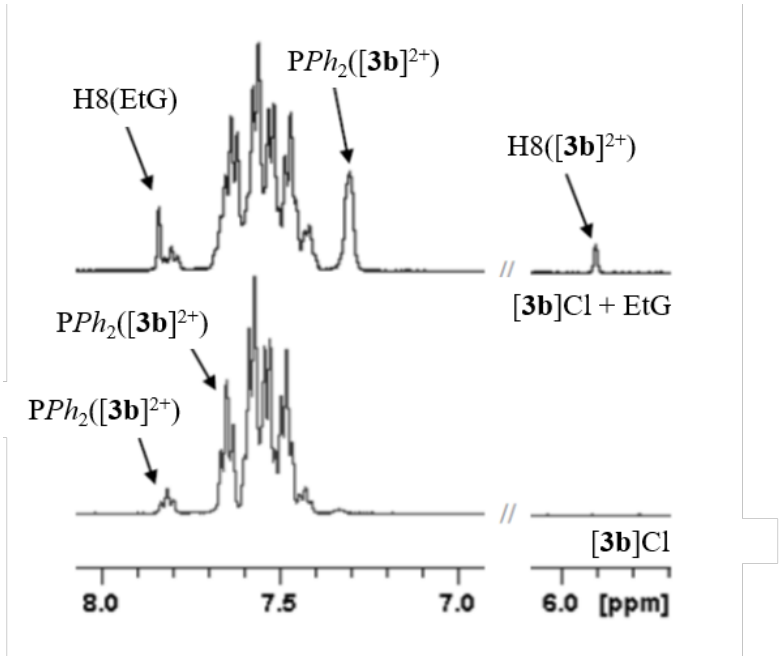

Figure S4. Guanosine H8 and phenyl region of the ^{1}H NMR spectra for **3b** (1 mM, bottom) and the reaction of **3b** (1 mM) with EtG (1 mM , top) after 24 h at 310 K. Approximately 25% of the aquated species reacted with EtG under the conditions employed.

A similar species is also observed in the reaction of **3b** with GMP ($\Delta\delta$(H8) = −1.87 ppm) for [Ru(GMP-N^7)(dppe)(*cis*-tach)], but to a lesser extent (~15%).

Viability Assays

The A549 cell line was kindly donated by The Bioscience Technology Facility, Department of Biology, University of York. The A2780 cell line was purchased from the ECACC. Cell cultures were maintained in a 5% humidified atmosphere of CO_2 at 37°C, in DMEM (A549) or RPMI 1640 (A2780) medium supplemented with 2 mM glutamine and 10% Foetal Bovine Serum. Culture medium and FBS were obtained from Invitrogen/Gibco and all other materials from Sigma.

Growth inhibition assays were performed using the MTT (3-(4,5-Dimethylthiazol-2-yl)-2,5-diphenyltetrazolium bromide) assay, with a modified procedure of Carmichael *et al*.[12] Cells were seeded at a density of 1,000 (A549) or 2,500 (A2780) cells per well in 100 μL of their respective culture medium in a flat bottomed 96 well plate (Corning). Positive controls consisted of culture medium with no cells, representative of 100% inhibition of MTT metabolism, and negative controls consisted of untreated cells, representative of 0% inhibition. A total of eight concentrations were tested, performed in octuplicate and typically between 0.1 μM and 300 μM, with the eight concentrations selected to fall on the dose-response curve for the compound.

The cells were incubated with the drug for 72 h before addition of MTT (50 μL, 2 mg/mL) in PBS and incubated for a further 2 h, over which MTT was metabolized to insoluble formazan crystals. The plates were centrifuged at 500 g for 10 minutes and 220 μL of the culture medium in each well was removed. The formazan was solubilised by addition of DMSO (150 μL). The value for each concentration of drug was plotted graphically as a percentage of the negative control compared to the positive. The data was fitted using a dose-response function and the concentration of drug to cause 50% reduction of the absorbance (compared to control values) was calculated as the IC_{50} value. IC_{50} values were calculated as the average of three independent experiments as the weighted mean.

A sample of **3c** in H_2O was observed to undergo a small change after 48 h. A new set of phenyl signals corresponding to approximately 5% of the phenyl resonance intensity was observed in the ^1H NMR spectrum alongside those of the chlorido and aqua/hydroxy complexes.

Table S2. IC_{50} measurements for compounds **1**, **2b** and **3a-i**.[a]

	IC_{50}[b] / μM	
Compound	A549	A2780
cisplatin	2.70 ± 0.05	0.43 ± 0.01
1	> 300	> 300
2b	> 300	> 300
3a	41.7 ± 1.0	12.4 ± 0.2
3b	9.88 ± 0.04	3.39 ± 0.12
3c	1.02 ± 0.03	0.35 ± 0.01
3d	1.15 ± 0.02	0.39 ± 0.01
3e	25.1 ± 0.4	7.47 ± 0.17
3f	2.73 ± 0.11	1.14 ± 0.04
3g	1.83 ± 0.66[c]	–
3h	11.81 ± 1.23[c]	–
3i	5.06 ± 1.01[c]	–

[a] Antiproliferative activities were determined by MTT assay and dose response curves are given in Figure S3 and S4. The IC_{50} calculated is the concentration of drug required for 50% growth inhibition over a 72-hour period. [b] Calculated as the average of triplicate experiments; error represents one standard deviation. [c] Errors represent standard deviation from 8 replicates.

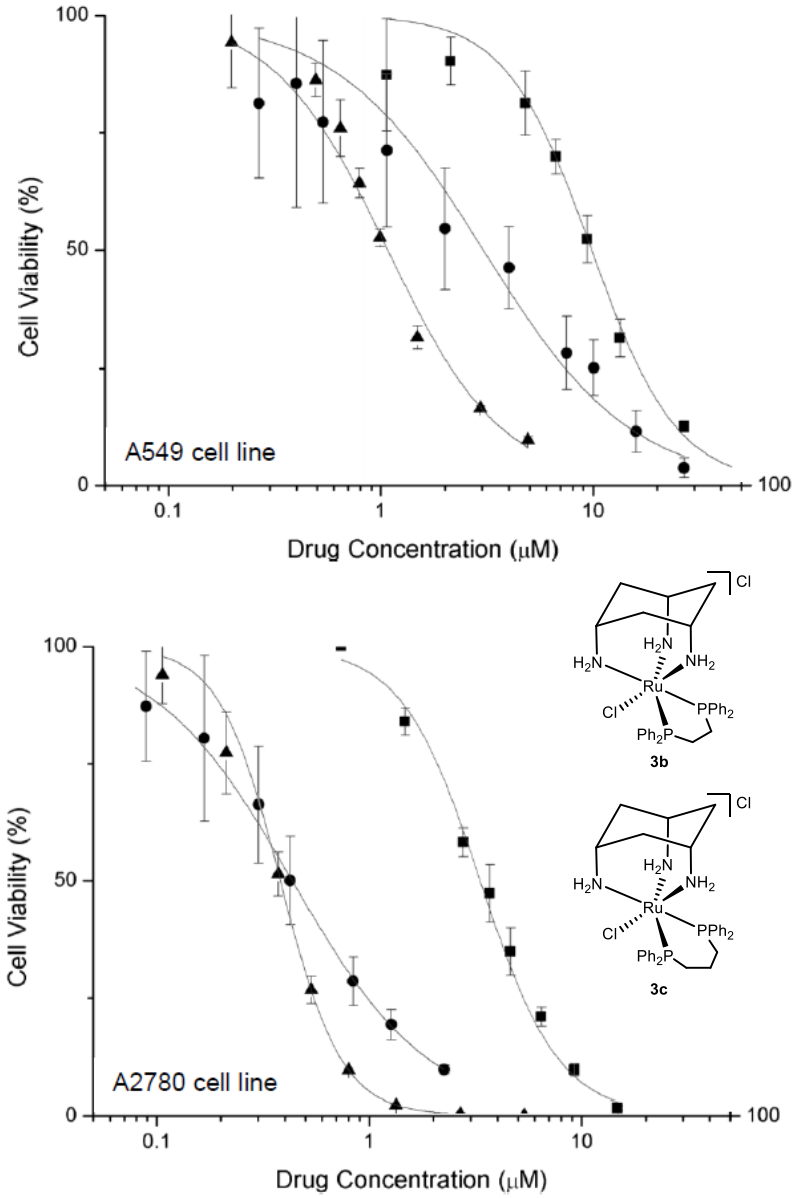

Figure S5. Representative dose response curves for cisplatin (●), **3b** (■) and **3c** (▲).

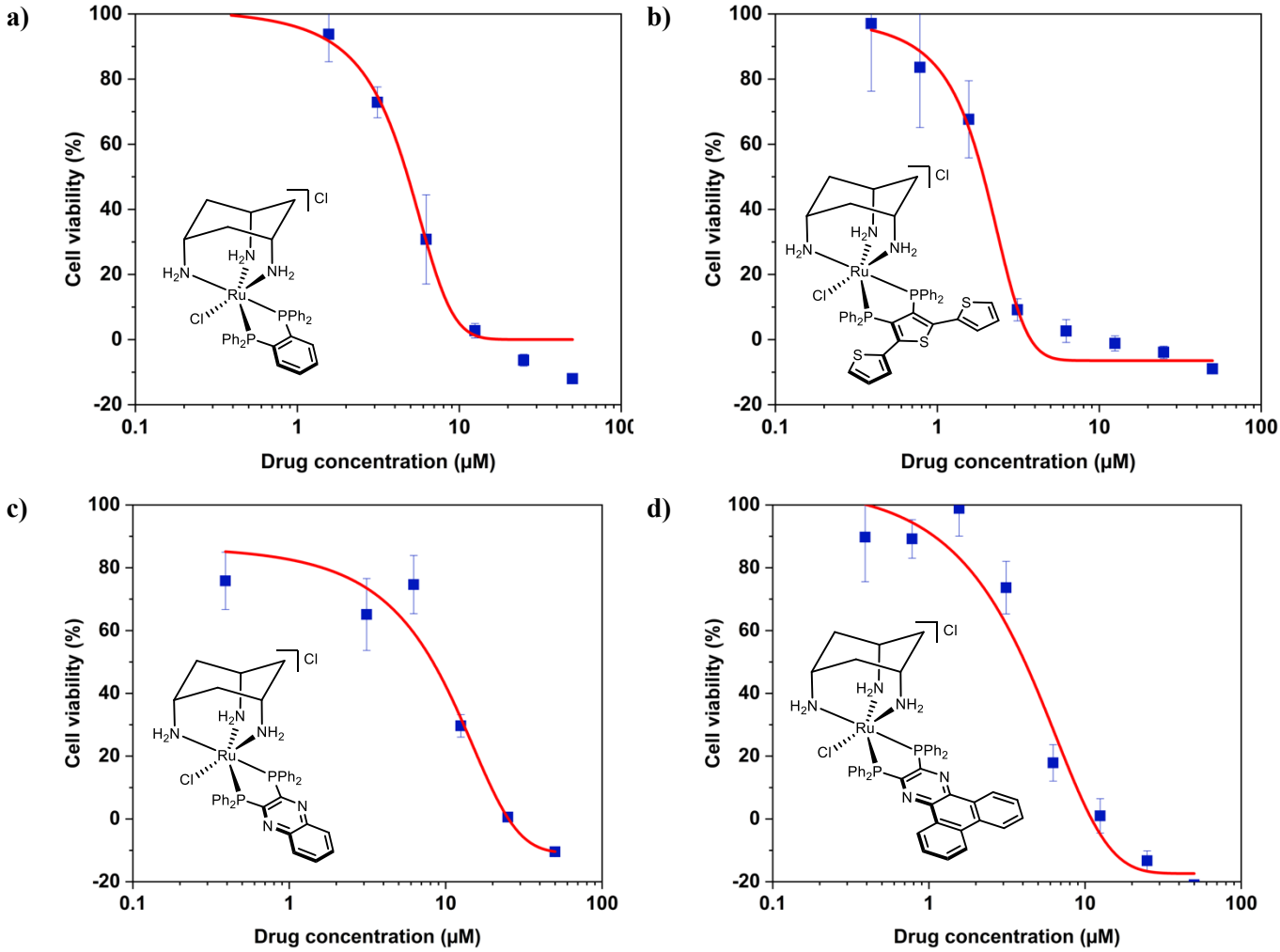

Figure S6. Representative dose response curves for A549 cells treated with a) **3f**, b) **3g**, c) **3h**, d) **3i**.

Competitive DNA Binding Studies

Solutions of CT-DNA and metal complex prepared in Tris-HCl buffer (5 mM), NaCl (30 mM), pH = 7.2. In a 96 well plate, CT-DNA (50 μM) and ethidium bromide (5 μM) were incubated for 1 hour in the dark. The complex was then titrated into the DNA-EB mixture. Before measurements, the solution was well mixed and incubated at room temperature for 5 min. Fluorescence spectra of EB bound to DNA were obtained at an excitation wavelength of 520 nm and an emission wavelength of 584 nm. Titrations were performed in triplicate, and the apparent binding constants were calculated using the Stern-Volmer equation:

$$\frac{I_0}{I} = 1 + K_{SV}[Q]$$

where I_0 and I are the fluorescence intensities of the DNA-EB adduct in the absence and presence of quencher respectively, K_{SV} is the Stern-Volmer quenching constant given by the slope of the plot and [Q] is the concentration of quencher. From these plots the apparent binding constants (K_{app}) are calculated from the equation:

$$K_{EB}[EB] = K_{app}[complex]$$

where $K_{EB} = 1x10^7\ M^{-1}$, [EB] is the concentration of EB (5 μM) and [complex] is the concentration of ruthenium complex which gave a 50% reduction of the initial emission intensity of EB.

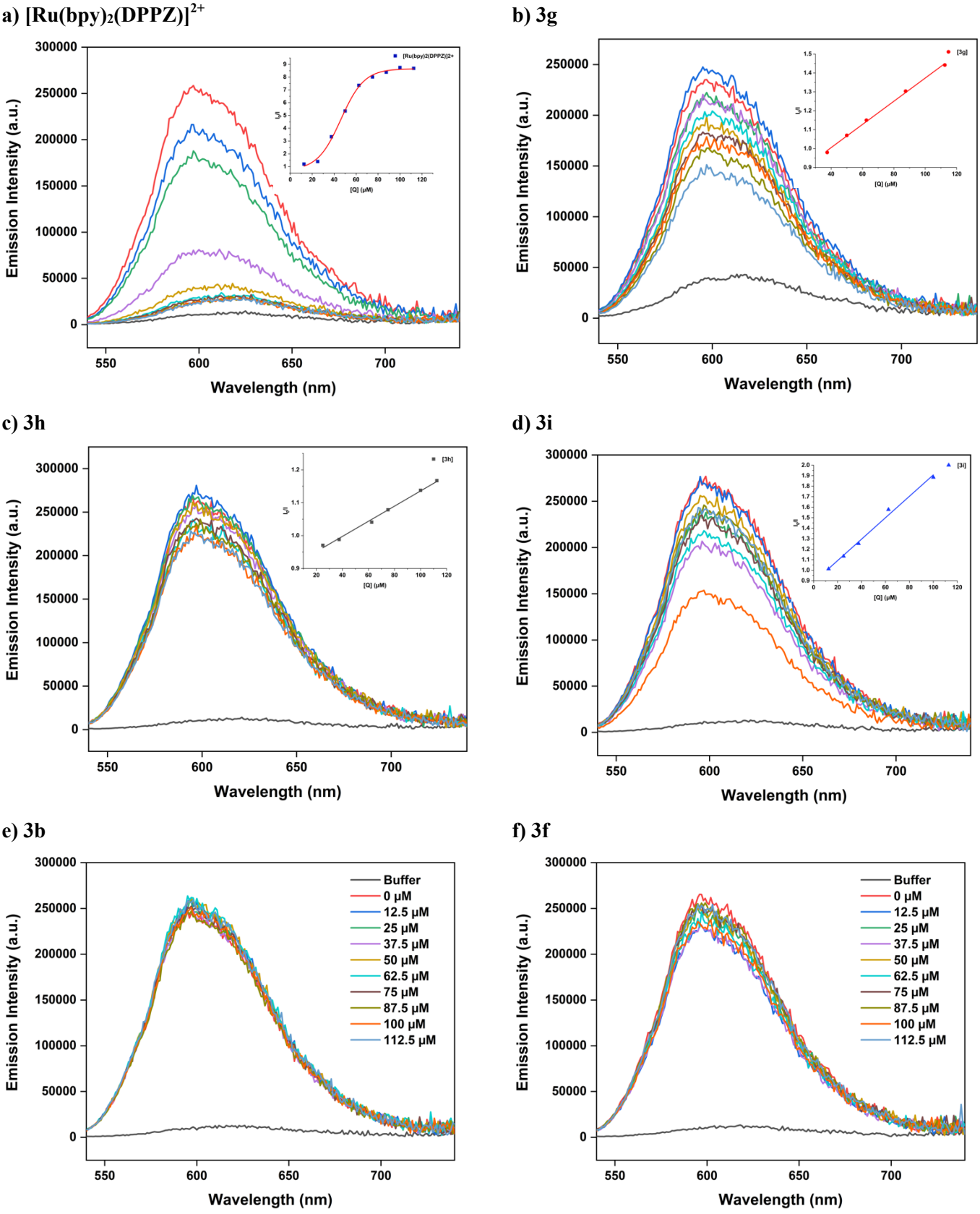

Figure S7. Fluorescence quenching of EB-DNA titration with a) $[Ru(bpy)_2(DPPZ)]^{2+}$, b) **3g**, c) **3h**, d) **3i**, e) **3b**, f) **3f**. [CT-DNA] = 5.0×10^{-5} M, [EB] = 5.0×10^{-6} M. Inset: Stern-Volmer plots.

FRET G-Quadruplex Assay

Fluorescence resonance energy transfer (FRET) melting assays were performed according to the procedure reported by De Cian and co-workers[13] on a Roche LightCycler 480 qPCR instrument. In these assays, the oligonucleotides of interest were obtained labelled at the 5' and 3' ends with FAM (a fluorescence donor) and TAMRA (a fluorescence quencher) respectively. In the folded state, proximity of the donor and quencher mean that FAM fluorescence is not observed since energy is transferred non-radiatively to TAMRA by FRET. As the temperature is raised and the secondary structure denatures, the fluorophores move further apart and hence the fluorescence signal increases. From the resulting curve, the characteristic melting temperature ($T_{1/2}$) is defined as that at which the normalised fluorescence signal equals 0.5. The change in melting temperature ($\Delta T_{1/2}$) induced by a small molecule ligand compared to that of the oligonucleotide in the absence of ligand provides an indication of the ligand's ability to stabilise the G4 structure.

The oligonucleotides (Eurogentec, Belgium) used were:

DNA model	Sequence
F21T (human telomeric G4)	5'-FAM-GGGTTAGGGTTAGGGTTAGGG-TAMRA-3'
FmycT (c-myc promoter G4)	5'-FAM-TTGAGGGTGGGTAGGGTGGGTAA-TAMRA-3'
F10T (duplex)	5'-FAM-TATAGCTATA-HEG-TATAGCTATA-TAMRA-3'

FAM = 6-carboxyfluorescein;

TAMRA = 6-carboxy-tetramethylrhodamine;

HEG = $[(-CH_2CH_2O-)_6]$

All sequences were annealed before use by heating for 2 minutes at 90 °C and then placed immediately into ice. The final concentration of oligonucleotide was 200 nM in all cases. The buffer used depended on the DNA model used. For F21T and F10T in K^+ conditions, 10 mM KCl, 90 mM LiCl and 10 mM Li cacodylate were used. For F21T in Na^+ conditions, the final buffer contained 100 mM NaCl, and 10 mM Li cacodylate. For FmycT in K^+ conditions, 1 mM KCl, 99 mM LiCl and 10 mM Li cacodylate were used. Ligand concentrations were either 0.5 μM or 1 μM. Appropriate control experiments were also carried out for each sample set. TMPyP4, tetra-(N-methyl-4-pyridyl)porphyrin tetra tosylate (used as a positive control), binds strongly to DNA quadruplexes by stacking on the G-tetrads at the core of the quadruplex, resulting in telomerase inhibition. Data processing was carried out using Origin 9, with $\Delta T_{1/2}$ used to represent ΔT_m.

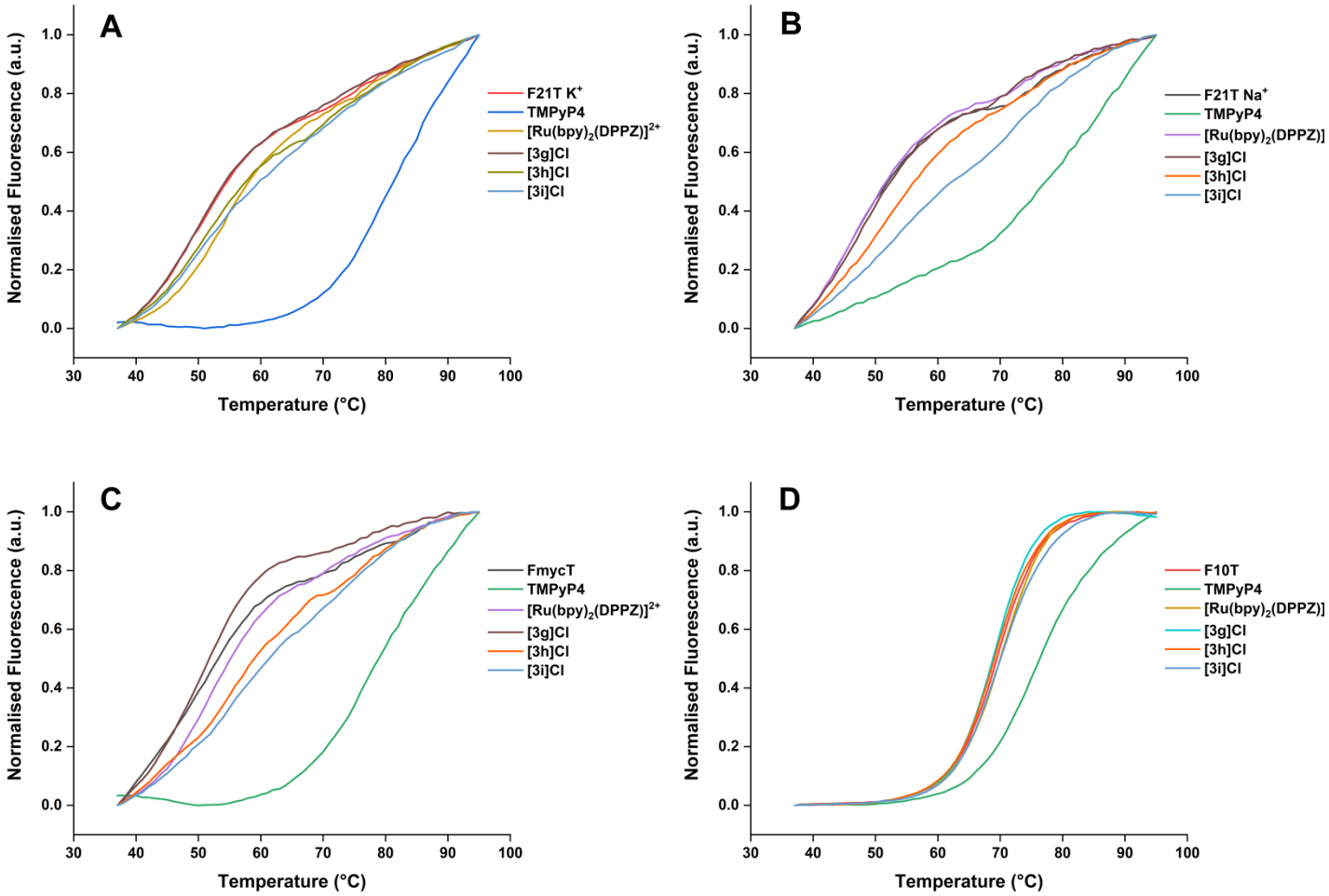

Figure S8. Representative thermal melting curves for A) F21T quadruplex (K^+ conditions); B) F21T quadruplex (Na^+ conditions); C) FmycT quadruplex (K^+ conditions); D) F10T duplex (K^+ conditions).

LiveCyte Cell Imaging

Cells were seeded at 1.6 x10^3 cells per well in a 96 well plate (Corning Costar) 24 h before adding compounds at the required concentrations. Immediately after adding compounds the plate was transferred to the LiveCyte (37 °C, 5% CO_2) for ptychographic quantitative phase imaging using the 10x objective, scanned 4 mm^2 field of view and time-lapse imaging for up to 4 days. Integrated image analysis software was used to extract changes in morphology, and dry mass of each cell over time. The summed mass of the cellular components excluding water, known as dry mass, was calculated for each cell population and used to measure the cell growth / proliferation.

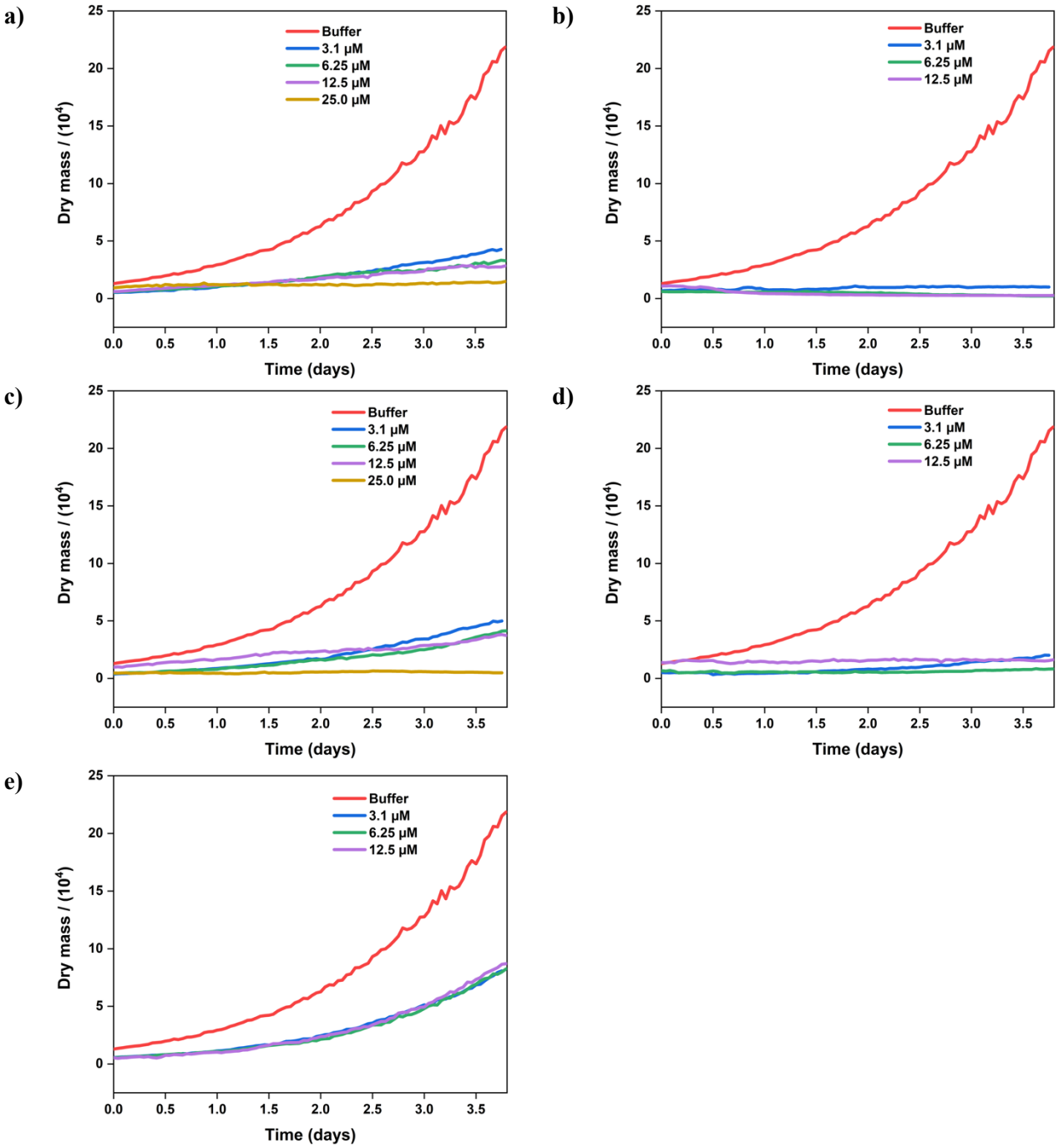

Figure S9. Representative dry mass plots for treatment of A549 cells with a) cisplatin, b) **3g**, c) **3h**, d) **3i**, e) **3f**.

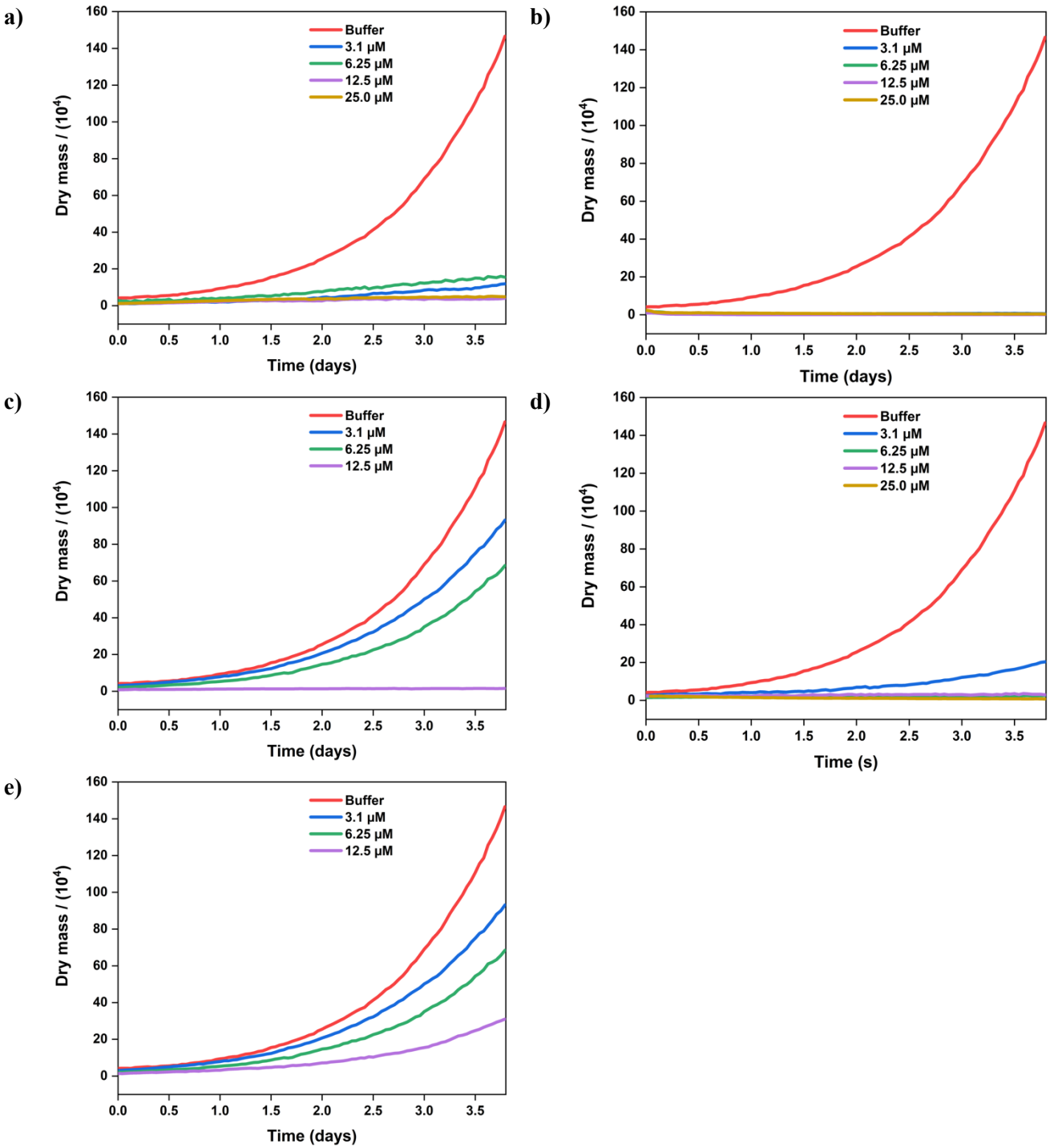

Figure S10. Representative dry mass plots for treatment of 293T cells with a) cisplatin, b) **3g**, c) **3h**, d) **3i**, e) **3f**.

The viability of A549 cells and 293T cells (Figures S11–13) was assessed by LiveCyte label-free time-lapse imaging.[14,15] Quantification of the total dry mass enables determination of cell death and cell growth. The effect of treatment with cisplatin, **3h**, **3g**, **3i** is clearly shown in the 0, 46 and 92-hour time-points. Reduction in the dry mass as the cell membrane ruptures is observed in treated wells.

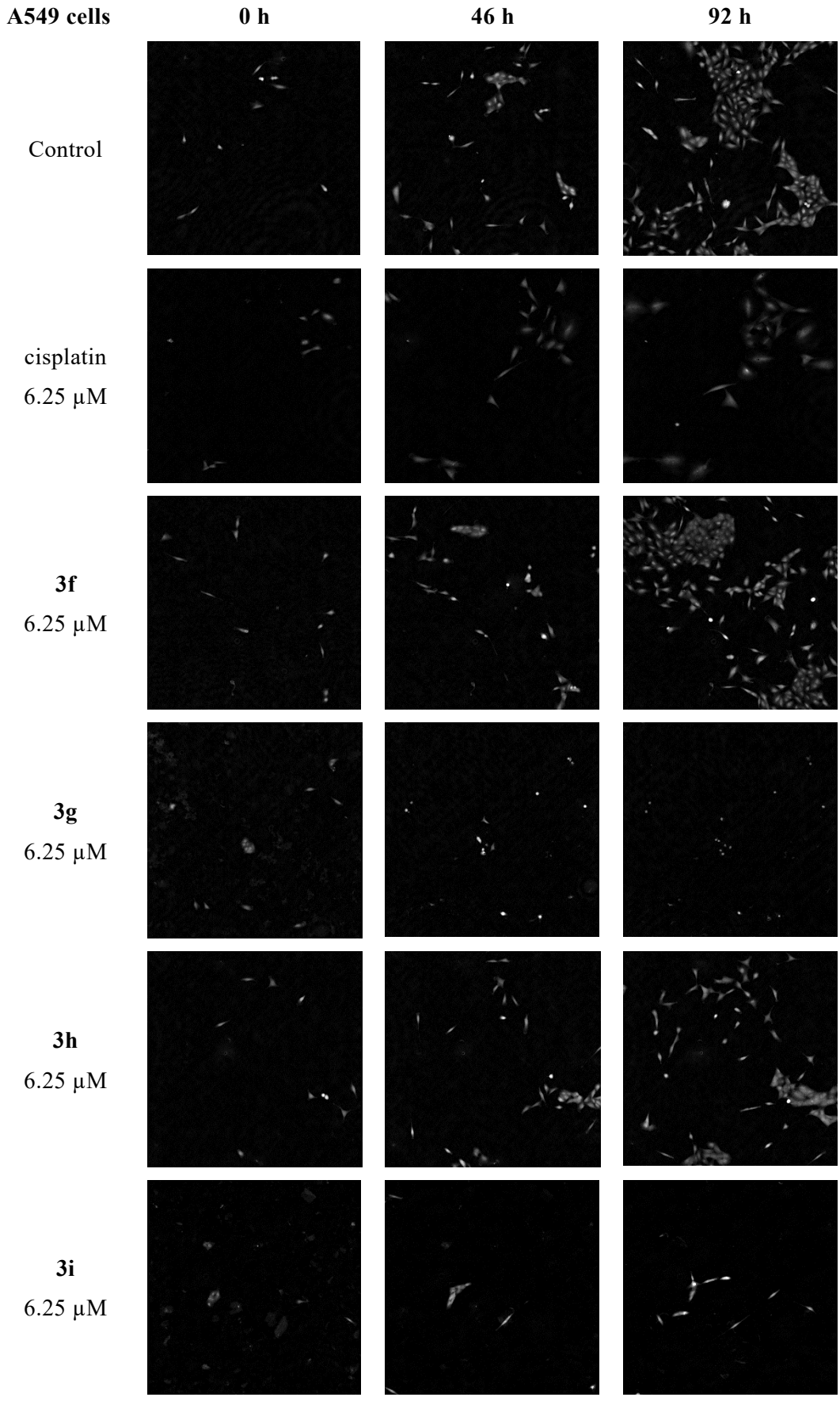

Figure S11. Time-lapse images of A549 cells treated with cisplatin and Ru *cis*-tach complexes.

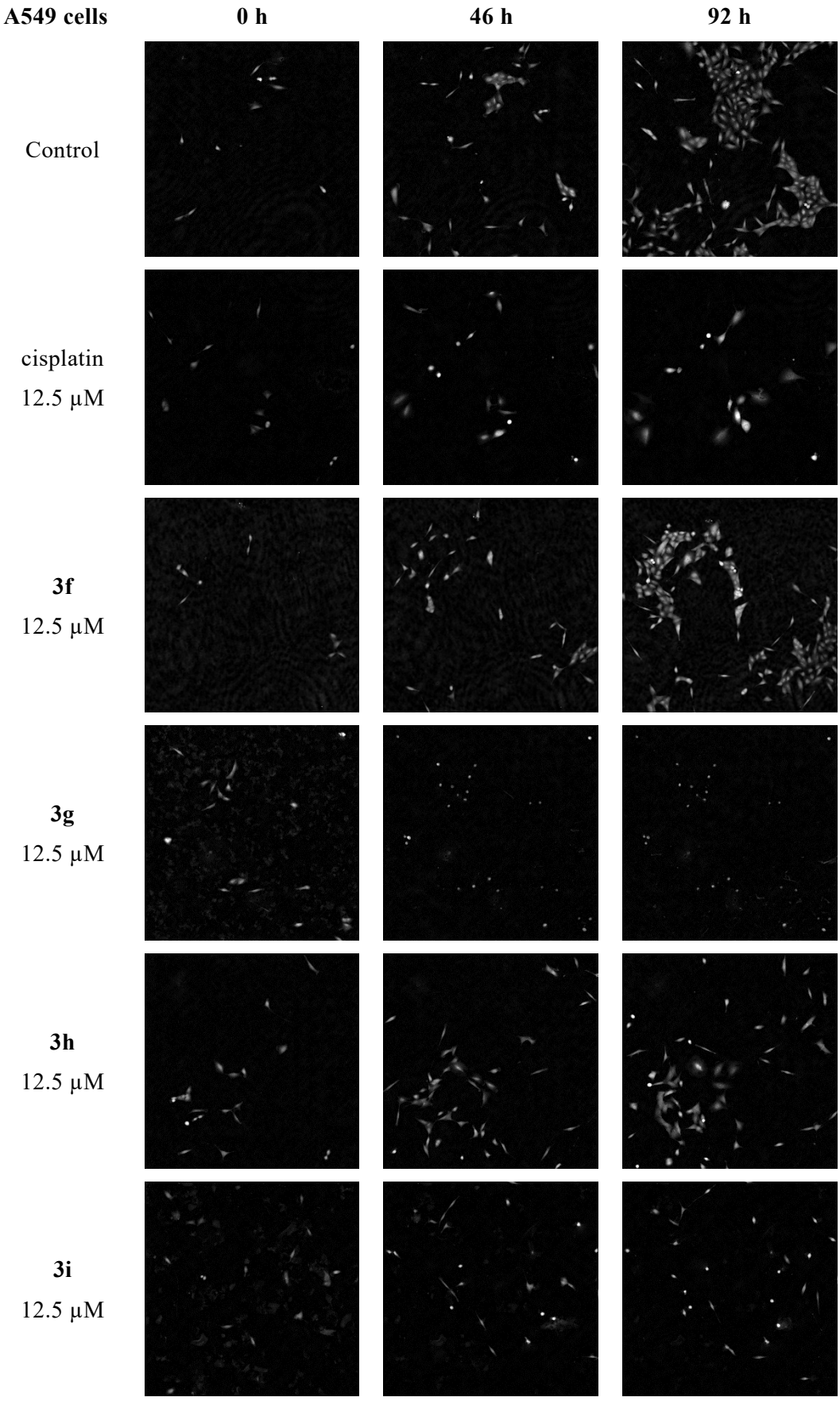

Figure S12. Time-lapse images of A549 cells treated with cisplatin and Ru *cis*-tach complexes.

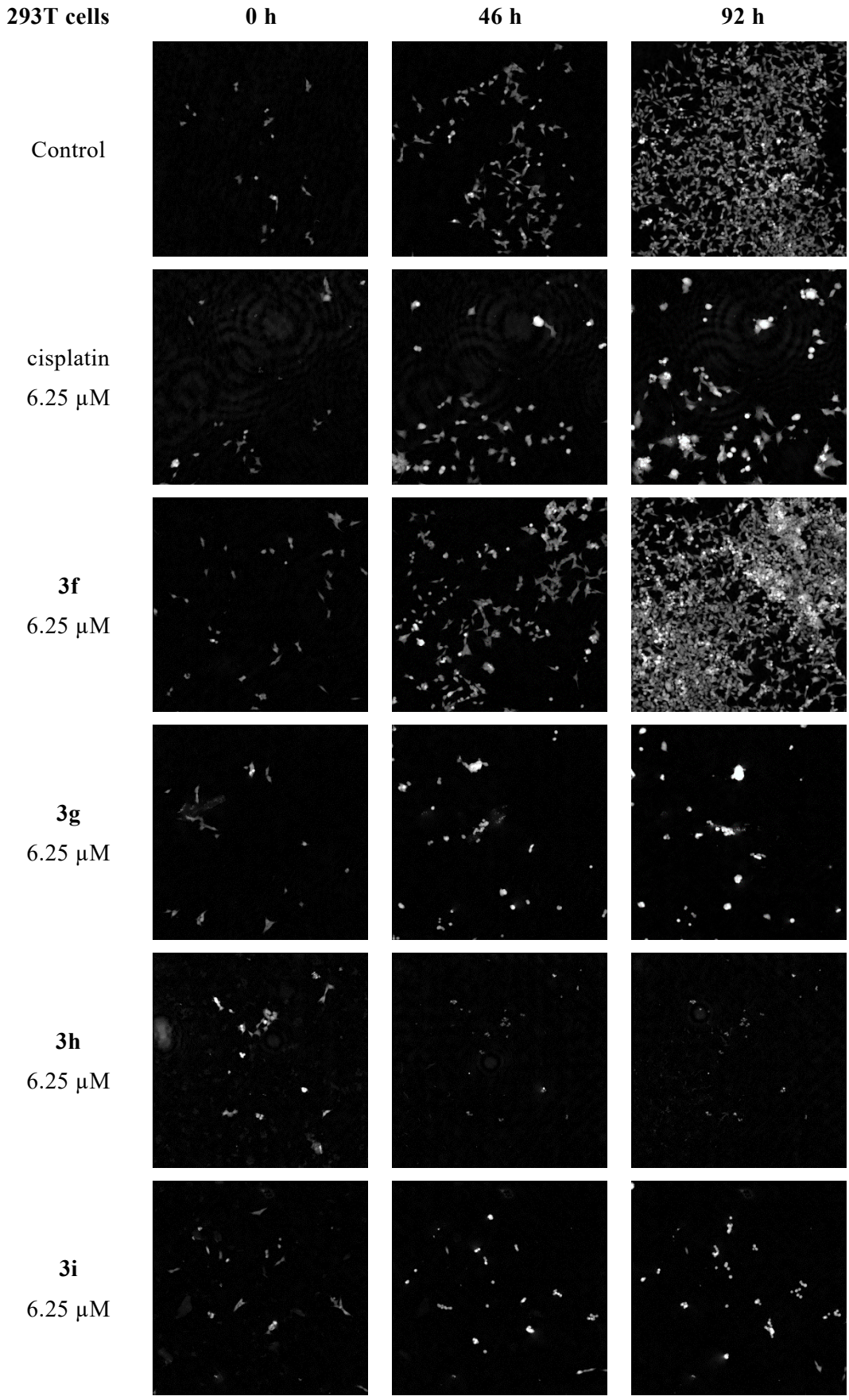

Figure S13. Time-lapse images of 293T cells treated with cisplatin and Ru *cis*-tach complexes.

X-Ray Crystallography

X-ray diffraction experiments on **[3h]PF_6** were carried out at 100(2) K on a Bruker APEX II CCD diffractometer using Mo-Kα radiation (λ = 0.71073 Å). Intensities were integrated in SAINT[16] and absorption corrections based on equivalent reflections were applied using SADABS. The structure was solved using ShelXT[17] all of the structures were refined by full matrix least squares against F^2 in ShelXL[17,18] using Olex2[19]. All of the non-hydrogen atoms were refined anisotropically. While all of the hydrogen atoms were located geometrically and refined using a riding model, apart from the N-H which were located in the difference map and refined with isotropic displacement parameters Uiso(H) = 1.5Ueq(N). All of the N-H distances were restrained to be the same. The PF_6^- counterion displayed disorder in the fluorine atom positions, the occupancies of the disordered F atoms were refined with their sum set to equal 1, restraints were applied to keep the P-F distances and F thermal parameters approximately the same. Crystal structure and refinement data are given in Table S1. Crystallographic data have been deposited with the Cambridge Crystallographic Data Centre as supplementary publication CCDC 1959465. Copies of the data can be obtained free of charge on application to CCDC, 12 Union Road, Cambridge CB2 1EZ, UK [fax(+44) 1223 336033, e-mail: deposit@ccdc.cam.ac.uk].

Table S3. Crystal data and structure refinement for [3h]PF_6

Empirical formula	$C_{38}H_{39}ClF_6N_5P_3Ru$
Formula weight	909.17
Temperature/K	100(2)
Crystal system	monoclinic
Space group	$P2_1/n$
a/Å	13.9014(6)
b/Å	19.6282(9)
c/Å	14.2188(6)
α/°	90
β/°	98.3870(10)
γ/°	90
Volume/Å^3	3838.2(3)
Z	4
ρ_{calc}g/cm^3	1.573
μ/mm^{-1}	0.669
F(000)	1848.0
Crystal size/mm^3	0.392 × 0.288 × 0.14
Radiation	MoKα (λ = 0.71073)
2θ range for data collection/°	3.562 to 55.748
Index ranges	-16 ≤ h ≤ 18, -25 ≤ k ≤ 25, -18 ≤ l ≤ 11
Reflections collected	34855
R_{int} / R_{sigma}	0.0518 / 0.0516
Data/restraints/parameters	9143/132/560
Goodness-of-fit on F^2	1.015
Final R indexes [I>=2σ (I)]	R_1 = 0.0350, wR_2 = 0.0695
Final R indexes [all data]	R_1 = 0.0534, wR_2 = 0.0762
Largest diff. peak/hole / e Å^{-3}	0.49/-0.55

References

1 I. P. Evans, A. Spencer and G. Wilkinson, *J. Chem. Soc. D*, 1973, 204–209.

2 S. C. Dhara, *Indian J. Chem*, 1970, 8, 193.

3 L. Cronin, S. P. Foxon, P. J. Lusby and P. H. Walton, *J. Biol. Inorg. Chem.*, 2001, **6**, 367–377.

4 K. Nagura, S. Saito, H. Yusa, H. Yamawaki, H. Fujihisa, H. Sato, Y. Shimoikeda and S. Yamaguchi, *J. Am. Chem. Soc.*, 2013, **135**, 10322–10325.

5 S. W. Hunt, L. Yang, X. Wang and M. G. Richmond, *J. Organomet. Chem.*, 2011, **696**, 1432–1440.

6 Y. Miura, H. Chiba, R. Katoono, H. Kawai, K. Fujiwara, S. Suzuki, K. Okada and T. Suzuki, *Tetrahedron Lett.*, 2012, **53**, 6561–6564.

7 A. J. Gamble, J. M. Lynam, R. J. Thatcher, P. H. Walton and A. C. Whitwood, *Inorg. Chem.*, 2013, **52**, 4517–4527.

8 F. Wang, H. Chen, S. Parsons, I. D. H. Oswald, J. E. Davidson and P. J. Sadler, *Chem. Eur. J.*, 2003, **9**, 5810–5820.

9 M. Jennerwein and P. A. Andrews, *Drug Metab. Dispos.*, 1995, **23**, 178–184.

10 C. Scolaro, C. G. Hartinger, C. S. Allardyce, B. K. Keppler and P. J. Dyson, *J. Inorg. Biochem.*, 2008, **102**, 1743–1748.

11 M. C. Lim and R. Bruce Martin, *J. Inorg. Nucl. Chem.*, 1976, **38**, 1911–1914.

12 J. Carmichael, J. B. Mitchell, W. G. Degraff, J. Gamson, A. F. Gazdar, B. E. Johnson, E. Glatstein and J. D. Minna, *Br. J. Cancer*, 1988, **57**, 540–547.

13 A. De Cian, L. Guittat, M. Kaiser, B. Saccà, S. Amrane, A. Bourdoncle, P. Alberti, M. P. Teulade-Fichou, L. Lacroix and J. L. Mergny, *Methods*, 2007, **42**, 183–195.

14 J. Marrison, L. Räty, P. Marriott and P. O'Toole, *Sci. Rep.*, 2013, **3**, 1–7.

15 R. Kasprowicz, R. Suman and P. O'Toole, *Int. J. Biochem. Cell Biol.*, 2017, 84, 89–95.

16 Bruker, SAINT+ v8.38A Integration Engine, Data Red.

17 G. M. Sheldrick, *Acta Crystallogr. Sect. C Struct. Chem.*, 2015, **71**, 3–8.

18 G. M. Sheldrick, *Acta Crystallogr. Sect. A Found. Crystallogr.*, 2007, **64**, 112–122.

19 O. V. Dolomanov, L. J. Bourhis, R. J. Gildea, J. A. K. Howard and H. Puschmann, *J. Appl. Crystallogr.*, 2009, **42**, 339–341.